

**ANALYTICAL AND EXPERIMENTAL INVESTIGATION OF A  
1/8-SCALE DYNAMIC MODEL OF THE  
SHUTTLE ORBITER**

**Volume I – Summary Report**

Prepared under Contract NAS 1-10635-12

for the

Langley Research Center  
National Aeronautics and Space Administration  
Hampton, Virginia 23365

by

P. W. Mason, H. G. Harris, J. Zalesak, and M. Bernstein

Grumman Aerospace Corporation  
Bethpage, New York 11714

May 1974

**ANALYTICAL AND EXPERIMENTAL INVESTIGATION OF A  
1/8-SCALE DYNAMIC MODEL OF THE  
SHUTTLE ORBITER**

**Volume I – Summary Report**

**Prepared under Contract NAS 1-10635-12**

**for the**

**Langley Research Center  
National Aeronautics and Space Administration  
Hampton, Virginia 23365**

**by**

**P. W. Mason, H. G. Harris, J. Zalesak, and M. Bernstein**

**Grumman Aerospace Corporation  
Bethpage, New York 11714**

**May 1974**

## ABSTRACT

A 1/8-scale structural dynamics model of the Space Shuttle Orbiter has been analyzed using the NASA Structural Analysis System (NASTRAN). Comparison of the calculated eigenvalues with preliminary test data for the unrestrained condition indicated that the analytical model was consistently stiffer, being about 20% higher in the first mode. The eigenvectors showed reasonably good agreement with test data. A series of analytical and experimental investigations undertaken to resolve the discrepancy are described. Modifications in the NASTRAN model based upon these investigations resulted in close agreement for both eigenvalues and eigenvectors.

### NOTE

This report is one of a series describing the Grumman effort in the NASA Langley Research Center 1/8-Scale Shuttle Structural Dynamics Model analysis program. The entire series of reports consists of:

- Orbiter
  - Task 12 NASA CR-132488 (Vol. I)
  - NASA CR-132489 (Vol. II)
  - NASA CR-132490 (Vol. IIIA)
  - NASA CR-132491 (Vol. IIIB)
- External Tank
  - Task 13 NASA CR-132549
- Solid Rocket Booster
  - Task 14 NASA CR-132492.

## FOREWORD

The work described in this report was carried out by the Grumman Aerospace Corporation, Bethpage, New York, as a subtask under the Master Agreement, Contract NAS1-10635, Task Order 12 with the Structural Mechanics Branch, Structures and Dynamics Division, NASA/Langley Research Center, Hampton, Virginia. The technical monitors were Mr. U. J. Blanchard and Mr. J. L. Sewall (alternate).

Many persons, both at Grumman and NASA/Langley (where the testing was conducted) have contributed to the various phases of this program. The following persons who contributed significantly to this effort are Grumman personnel unless noted otherwise:

- Management: E. F. Baird, M. Bernstein
- Design: A. P. LaValle, P. W. Tracy, F. L. Halfen, C. M. Cacho-Negrete, P. J. Cartensen, and S. Rosenstein
- Stress Analysis: W. P. Bierds
- NASTRAN Dynamic Analysis: P. W. Mason, J. Zalesak, D. Gregory, M. Bernstein, R. Coppolino, and A. Levy
- Experimental Investigation: U. J. Blanchard, L. D. Pinson, and S. A. Leadbetter (all of NASA/Langley)  
J. Barrett (Rockwell International)  
M. Bernstein, J. E. Flynn, and A. I. Miller
- Correlation and Re-analysis: M. Bernstein, W. Lansing, H. G. Harris, P. W. Mason, A. I. Miller, J. Zalesak, J. E. Flynn, E. M. Bauer  
L. D. Pinson, J. L. Sewall (both of NASA/Langley)  
J. Barrett (Rockwell International)
- Nonlinear Imperfect Solutions: E. Saleme and H. Armen, Jr.

## VOLUME I TABLE OF CONTENTS

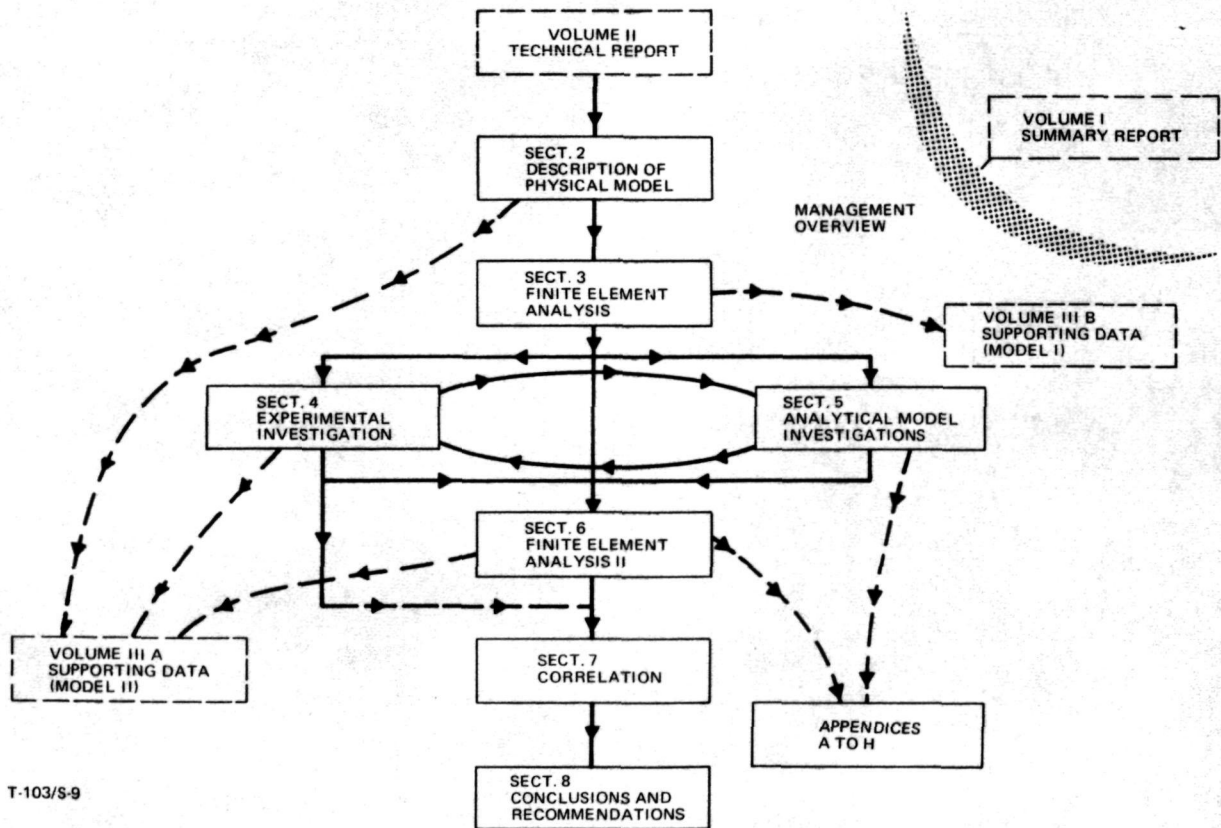
	<u>Page</u>
Introduction . . . . .	1
Symbols and Abbreviations. . . . .	3
Description of Prototype Shuttle . . . . .	5
Description of 1/8-Scale Model . . . . .	5
NASTRAN Finite Element Models . . . . .	11
Experimental Results . . . . .	16
Comments on the NASTRAN System. . . . .	20
Flexibility of the NASTRAN System. . . . .	20
Capability of NASTRAN . . . . .	21
Conclusions . . . . .	22
References . . . . .	24

## VOLUME I LIST OF ILLUSTRATIONS

<u>Figure</u>		<u>Page</u>
1	Grumman Parallel-Burn Space Shuttle Design 619 Used as Reference Prototype for 1/8-Scale Model Design . .	6
2	Prototype Orbiter (Grumman Design 619) Structural Arrangement . . . . .	7
3	Mockup of 1/8-Scale Shuttle Model Basic Configuration . . .	9
4	1/8-Scale Orbiter Model Structural Configuration . . . . .	10
5	Mode Survey of Model in Upside-Down Suspended Position .	16
6	General View of Static Load Testing Arrangement of 1/8-Scale Orbiter Model . . . . .	17
7	Load Vs Deflection Curves for $\pm Z$ Load on Nose Bulkhead .	18

3, 4, and 5; this second model, and its associated analytical results, is referred to as "Model II"

- Section 7 correlates test and analytical results
- Section 8 provides conclusions and recommendations regarding the overall study task
- Appendixes A through H provide detailed discussions of supporting data for the main sections of the report
- Volume IIIA - Supporting Data: Design drawings for the 1/8-Scale Orbiter Model, static test data, and the NASTRAN Model II finite element idealization, input data, and detailed analytical results
- Volume IIIB - Supporting Data: NASTRAN Model I finite element idealization, input data, and detailed analytical results.



T-103/S-9

Relationship Between 1/8-Scale Orbiter Model Tasks and Sections of this Report

## VOLUME I TABLE OF CONTENTS

	<u>Page</u>
Introduction . . . . .	1
Symbols and Abbreviations. . . . .	3
Description of Prototype Shuttle . . . . .	5
Description of 1/8-Scale Model . . . . .	5
NASTRAN Finite Element Models . . . . .	11
Experimental Results . . . . .	16
Comments on the NASTRAN System. . . . .	20
Flexibility of the NASTRAN System. . . . .	20
Capability of NASTRAN . . . . .	21
Conclusions . . . . .	22
References . . . . .	24

## VOLUME I LIST OF ILLUSTRATIONS

<u>Figure</u>	<u>Page</u>	
1	Grumman Parallel-Burn Space Shuttle Design 619 Used as Reference Prototype for 1/8-Scale Model Design . . . . .	6
2	Prototype Orbiter (Grumman Design 619) Structural Arrangement . . . . .	7
3	Mockup of 1/8-Scale Shuttle Model Basic Configuration . . . . .	9
4	1/8-Scale Orbiter Model Structural Configuration . . . . .	10
5	Mode Survey of Model in Upside-Down Suspended Position . . . . .	16
6	General View of Static Load Testing Arrangement of 1/8-Scale Orbiter Model . . . . .	17
7	Load Vs Deflection Curves for $\pm Z$ Load on Nose Bulkhead . . . . .	18

VOLUME I LIST OF TABLES

<u>No.</u>		<u>Page</u>
1	Summary of Significant Scale Factors . . . . .	8
2	Statistical Description of 1/8-Scale Orbiter Model I . . . . .	11
3	Component Weights (1/2 Model) . . . . .	11
4	Calculated Maximum Deflections for Typical Panels Under Own Weight with Various Boundary Conditions . . . . .	13
5	Comparison of Analytical and Preliminary Experimental Results for the Symmetric Free-Free Normal Modes . . . . .	14
6	Comparison of Analytical and Experimental Results for the Antisymmetric Free-Free Modes . . . . .	15
7	Weight Comparison of Grumman Design 619 Prototype and 1/8-Scale Model . . . . .	15
8	Comparison of Prototype and 1/8-Scale Model Dynamic Analyses with Test Results for Symmetric Free-Free Modes . . . . .	15
9	1/8-Scale Orbiter Model - Influence Coefficients . . . . .	19



## VOLUME II TABLE OF CONTENTS

<u>Section</u>		<u>Page</u>
1	INTRODUCTION . . . . .	1-1
	1.1 Overview and Summary . . . . .	1-1
	1.2 Symbols and Abbreviations . . . . .	1-4
2	DESCRIPTION OF PHYSICAL MODEL . . . . .	2-1
	2.1 Design Objective . . . . .	2-1
	2.2 Design Considerations . . . . .	2-1
	2.2.1 Similitude Requirements . . . . .	2-1
	2.2.2 Loads . . . . .	2-7
	2.2.3 Mass and Stiffness Distribution. . . . .	2-7
	2.3 Fabrication Details . . . . .	2-14
	2.3.1 Fuselage . . . . .	2-14
	2.3.2 Wings . . . . .	2-16
	2.3.3 Vertical Fin . . . . .	2-18
	2.3.4 Cargo Doors . . . . .	2-18
	2.3.5 Payload, Ballast Weights, Attachments and Other Details . . . . .	2-18
3	FINITE ELEMENT ANALYSIS PROCEDURES . . . . .	3-1
	3.1 Basic Philosophy . . . . .	3-1
	3.2 Overall Analysis Flow . . . . .	3-2
	3.3 Substructuring Procedure . . . . .	3-5
	3.4 Finite Elements Model I . . . . .	3-8
	3.5 Mass Data . . . . .	3-18
	3.6 Component Results for Model I . . . . .	3-20
	3.7 Orbiter Results for Model I . . . . .	3-23
4	EXPERIMENTAL INVESTIGATION . . . . .	4-1
	4.1 Testing Procedures . . . . .	4-1
	4.2 Mode Survey with Orbiter Model Suspended Horizontally at Interstage Points . . . . .	4-1
	4.3 Mode Survey with Orbiter Model Suspended at Fuselage Nose . . . . .	4-9
	4.4 Static Tests . . . . .	4-14

VOLUME II TABLE OF CONTENTS (Cont)

<u>Section</u>		<u>Page</u>
5	ANALYTICAL MODEL INVESTIGATION . . . . .	5-1
5.1	Background . . . . .	5-1
5.2	Substructure Contributions to the Generalized Mass and Stiffness . . . . .	5-2
5.3	Adequacy of the CQDMEM2 Element . . . . .	5-7
5.4	Fuselage EI Curves . . . . .	5-9
5.5	Dynamic Analysis of Beam Models . . . . .	5-13
5.6	Evaluation of the Guyan Reduction Procedure . . . . .	5-18
5.7	Forward Fuselage Investigation . . . . .	5-25
5.8	Stress Distributions . . . . .	5-31
5.9	Linear Buckling Analysis . . . . .	5-36
5.10	Effect of Initial Imperfections on Panel Stiffness . . . . .	5-40
5.11	Evaluation of Test Data . . . . .	5-52
	5.11.1 Preload . . . . .	5-52
	5.11.2 Strains . . . . .	5-55
	5.11.3 Influence Coefficients . . . . .	5-57
5.12	Effectiveness of Door Attachments . . . . .	5-59
	5.12.1 Symmetric Bending Case . . . . .	5-59
	5.12.2 Antisymmetric Behavior Case . . . . .	5-64
6	FINITE ELEMENT ANALYSIS FOR MODEL II . . . . .	6-1
6.1	Finite Elements Model II . . . . .	6-1
	6.1.1 General . . . . .	6-1
	6.1.2 Remodeling Guide Lines . . . . .	6-2
	6.1.3 Fuselage . . . . .	6-3
	6.1.4 Wing . . . . .	6-9
	6.1.5 Fin . . . . .	6-11
	6.1.6 Cargo Doors . . . . .	6-13
	6.1.7 Payload . . . . .	6-14
6.2	NASTRAN Analysis for Model II . . . . .	6-15
	6.2.1 Component Results . . . . .	6-15
	6.2.2 Orbiter Results . . . . .	6-16

VOLUME II TABLE OF CONTENTS (Cont)

<u>Section</u>	<u>Page</u>
7	<b>CORRELATION OF ANALYTICAL AND EXPERIMENTAL RESULTS . . . . .</b> 7-1
7.1	Static Test Correlation . . . . . 7-1
7.2	Dynamic Test Correlation . . . . . 7-17
8	<b>CONCLUSIONS AND RECOMMENDATIONS . . . . .</b> 8-1
8.1	Modeling Procedures . . . . . 8-1
8.2	Correlation. . . . . 8-1
8.3	Comments on and Experience with NASTRAN. . . . . 8-2
	8.3.1 Flexibility of the NASTRAN System. . . . . 8-2
	8.3.2 Capability of NASTRAN . . . . . 8-3
	8.3.3 Comparison of Computer Running Times . . . . . 8-5
9	<b>REFERENCES . . . . .</b> 9-1
 <u>Appendixes</u>	
A	Finite Element Model I . . . . . A-1
B	Orbiter Static Test Cases - Analytical Deflections for Model I Supported on Interstages . . . . . B-1
C	Mode Survey Data. . . . . C-1
D	Error Bounds for Approximate Frequencies of Free-Free Undamped Vibration Systems . . . . . D-1
E	Large Deflection Behavior of Initially Imperfect Rectangular Plates Under Uniform End-Shortening and Extension . . . . . E-1
F	Model II Fuselage and Wing Cover Effective Width Calculations . . . . . F-1
G	Test Results Which Form the Basis for Modification of Model I . . . . . G-1
H	Orbiter Static Test Case Analytical Deflections for Model II. . . . . H-1

## VOLUME II LIST OF ILLUSTRATIONS

<u>Figure</u>		<u>Page</u>
2-1	Grumman Parallel-Burn Space Shuttle Design 619 Used as Reference Prototype for 1/8-Scale Model Design . . . . .	2-2
2-2	Mockup of 1/8-Scale Shuttle Model Basic Configuration . . . . .	2-3
2-3	Prototype Orbiter (Grumman Design 619) Structural Arrangement . . . . .	2-4
2-4	Views of Finished 1/8-Scale Orbiter Model . . . . .	2-5
2-5	Fuselage "Stick Model" Mass Distribution (One-Half Structure). . . . .	2-9
2-6	Comparison of Cross-Sectional Areas of Prototype and 1/8-Scale Orbiter Model . . . . .	2-10
2-7	Comparison of Fuselage Moments of Inertia of Prototype and 1/8-Scale Orbiter Model . . . . .	2-11
2-8	Dead Load Shear and Moment Diagram for the 1/8-Scale Orbiter Model Supported at the Interstage (Half Orbiter Values). . . . .	2-12
2-9	Axial Load and Moment Diagrams for the 1/8-Scale Orbiter Model Hung from Nose Fitting (Half Orbiter Values) . . . . .	2-13
2-10	Fuselage of 1/8-Scale Orbiter Model During Fabrication . . . . .	2-15
2-11	Details of the Forward Fuselage Module. . . . .	2-15
2-12	Forward-To-Mid-Fuselage Interface . . . . .	2-15
2-13	Aft Fuselage Details . . . . .	2-16
2-14	Aft Fuselage - Engine Mounts . . . . .	2-16
2-15	Construction of 1/8-Scale Orbiter Model Wing . . . . .	2-17
2-16	Fuselage Sidewall and Wing Shear Attachments . . . . .	2-17
2-17	Fin Structure . . . . .	2-19
2-18	Fin Forward Attachment Detail . . . . .	2-19
2-19	Cargo Doors During Assembly . . . . .	2-19
2-20	Cargo Door Attachment Details . . . . .	2-20

VOLUME II LIST OF ILLUSTRATIONS (Cont)

<u>Figure</u>		<u>Page</u>
2-21	Location of Main Ballast Weights . . . . .	2-21
2-22	Payload Typical Attachment Details . . . . .	2-21
3-1	Schematic Diagram of Overall Analysis Flow . . . . .	3-3
3-2	Flow Diagram for NASTRAN Substructuring to Obtain Normal Modes . . . . .	3-7
3-3	Basic Assumptions Used in Developing the Warped Quadrilateral "CQDMEM 2" Finite Element . . . . .	3-10
3-4	Behavior of a Beam Segment Composed of Four CQDMEM 2 Elements and Two Rods . . . . .	3-11
3-5	Alternate Rod and Shear Panel Idealization for Fuselage Side wall . . . . .	3-11
3-6	Error Associated with Coarseness of Grid . . . . .	3-13
3-7	Error in Strain Energy by Assuming Constant Stress in Cap Members . . . . .	3-13
3-8	Schematic of Cargo Door Frames . . . . .	3-15
3-9	NASTRAN Plot of Orbiter Fuselage . . . . .	3-15
3-10	NASTRAN Plot of Wing Rib and Spar Shear Webs . . . . .	3-16
3-11	NASTRAN Plot of Wing Top Cover . . . . .	3-16
3-12	NASTRAN Plot of Fin Webs . . . . .	3-17
3-13	NASTRAN Plot of Fin Cover . . . . .	3-17
3-14	NASTRAN Plot of Cargo Bay Door Covers . . . . .	3-18
3-15	Model Weight Data . . . . .	3-19
3-16	Orbiter Phase 2 Degrees-Of-Freedom Model I (Two sheets). . . . .	3-21
3-17	First Symmetric Mode . . . . .	3-24
3-18	Second Symmetric Mode . . . . .	3-25

VOLUME II LIST OF ILLUSTRATIONS (Cont)

<u>Figure</u>		<u>Page</u>
4-1	Orbiter Model Suspended in Horizontal Inverted Attitude for Vibration Tests - Forward View . . . . .	4-2
4-2	Orbiter Model Suspended in Horizontal Inverted Attitude for Vibration Tests - Aft View . . . . .	4-2
4-3	Orbiter Model Suspended in Vertical Attitude for Vibration Tests With Axial Preload. . . . .	4-3
4-4	Suspension Cable Connections and Typical Shaker Installation Used for Vibration Tests of Orbiter Model in Vertical Attitude . . . . .	4-4
4-5	Linkage for Applying Axial Preload to Fuselage During Vibration Tests of Orbiter Model Suspended in Vertical Attitude . . . . .	4-5
4-6	Typical Strain Gage Installation on Orbiter Model Fuselage Side Wall Panels and Longerons . . . . .	4-6
4-7	Location of Strain and Dial Gages for Static Tests . . . . .	4-7
4-8	Location of Strain Gages - Section View. . . . .	4-8
4-9	Load-Strain Curves for Side Wall Panels (Sta 99.0) . . . . .	4-10
4-10	Load-Strain Curves for Side Wall Panels (Sta 110.0) . . . . .	4-11
4-11	Load-Strain Curves for Bottom Deck Panels (Sta 110.0) . . . . .	4-12
4-12	Load-Strain Curves for Side Wall Panel (Sta 122.0) . . . . .	4-13
4.13	Load-Strain Curves for Longerons (Sta 116.0) . . . . .	4-13
4-14	Details of Model Support for Static Tests . . . . .	4-14
4-15	Static Test Setup (Side View) . . . . .	4-15
4-16	Static Test Set Up (Front View) . . . . .	4-16
4-17	Apparatus for Loading and Measurements at Aft End of Fuselage During Static Tests . . . . .	4-17
4-18	Dial Gages Used for Measurement of Forward Cabin Ballast Deflection During Static Tests . . . . .	4-18

VOLUME II LIST OF ILLUSTRATIONS (Cont)

<u>Figure</u>		<u>Page</u>
4-19	Load-Deflection Curves for $\pm Z$ Loading on Nose Bulkhead (Sta 46.75) . . . . .	4-21
4-20	Load-Deflection Curves for $\pm Z$ Loading at Mid-Fuselage (Sta 119) . . . . .	4-21
5-1	Relationships Among Various Analytical Investigations Discussed in Section 5 . . . . .	5-3
5-2	Comparison of Flexibilities for a Pure Bending Couple Applied to Square Membrane Elements $l = h$ . . . . .	5-7
5-3	Fuselage Side Wall in Pure Bending. . . . .	5-8
5-4	1/8-Scale Orbiter Fuselage Beam Model . . . . .	5-10
5-5	1/8-Scale Orbiter Fuselage Vertical Deflections for Unit Moment at Fin Ballast Center of Gravity (Model I Analysis) . . . . .	5-11
5-6	1/8-Scale Orbiter Fuselage Model - Moment of Inertia . . . . .	5-12
5-7	1/8-Scale Orbiter Fuselage Model - Position of Computed Neutral Axis . . . . .	5-14
5-8	Elevation of Aft Fuselage and Fin . . . . .	5-15
5-9	1/8-Scale Aft Fuselage Model-Horizontal Deflections . . . . .	5-16
5-10	1/8-Scale Shuttle Beam Model - First Three Modes for Fuselage Symmetric Case . . . . .	5-17
5-11	Simple Two-DOF Problem . . . . .	5-20
5-12	Idealized Forward Steel Ballast . . . . .	5-26
5-13	Actual Forward Steel Ballast . . . . .	5-26
5-14	Cantilevered Forward Fuselage (First Mode) . . . . .	5-27
5-15	Forward Fuselage First Symmetric Mode - Model I Orbiter Analysis . . . . .	5-28
5-16	Forward Fuselage First Symmetric Mode - Model I Orbiter Analysis Relative to Sta 87.5 (53.24 Hz). . . . .	5-28
5-17	Cantilevered Forward Fuselage, Case 2 (First Mode) . . . . .	5-30

VOLUME II LIST OF ILLUSTRATIONS (Cont)

<u>Figure</u>		<u>Page</u>
5-18	Cantelevered Forward Fuselage, Case 3 (First Mode) . . . . .	5-30
5-19	Orbiter Model 1-g Moments Diagram (Half Structure Values) . . . . .	5-32
5-20	NASTRAN Model I 1-g Stresses and Cap Loads . . . . .	5-33
5-21	Comparison of 1-g and Critical Buckling Stresses for Bottom Deck Panels - Orbiter Suspended Inverted from Interstage Fittings . . . . .	5-38
5-22	Comparison of 1-g and Critical Buckling Stresses for Fuselage Side Wall Panels - Orbiter Suspended Upside- Down from Interstage Fittings . . . . .	5-38
5-23	Stress Variation in One Cycle for a 9-1/2 x 12-1/2-Inch Bottom Deck Panel Located in the Mid-Fuselage Region . . . . .	5-39
5-24	Plate Behavior Under Compressive Load . . . . .	5-41
5-25	Von-Kármán Model of the Effective Width of a Post- Buckled Plate . . . . .	5-41
5-26	Typical Behavior of an Initially Perfect Plate Loaded in Compression. . . . .	5-44
5-27	Load-Strain Curves for Square Plate with Various Initial Imperfections . . . . .	5-46
5-28	Load vs End Shortening for Typical Side Wall Panel . . . . .	5-47
5-29	Load vs End Shortening for Typical Bottom Deck Panel . . . . .	5-48
5-30	Load vs End Shortening for Typical Wing Cover Panel . . . . .	5-49
5-31	Variation of Effectiveness Factor With Aspect Ratio . . . . .	5-51
5-32	Effect of Axial Load on Frequency . . . . .	5-52
5-33	Axial and Bending Strains . . . . .	5-56
5-34	Strain-Curvature Relations . . . . .	5-56
5-35	Assumed Shapes of Panel Imperfections. . . . .	5-56
5-36	Moment of Inertia for Fuselage and Effective Door Longeron at Sta 116.0 . . . . .	5-60



VOLUME II LIST OF ILLUSTRATIONS (Cont)

<u>Figure</u>		<u>Page</u>
5-37	Door Longeron Properties . . . . .	5-62
5-38	Simplified NASTRAN Model Incorporating Changes to Model I (One-Quarter of Door Region Shown) . . . . .	5-62
5-39	Door-Fuselage Strap . . . . .	5-63
5-40	Door-Fuselage Connection . . . . .	5-63
5-41	Simplified NASTRAN Model Results . . . . .	5-63
5-42	Torque Cell Representation of Typical Fuselage Section . . . . .	5-64
5-43	Equivalent Shear Panel to Represent Energy in Door and Fuselage Longerons Plus Physical Door Shell Extension (Model I Simulation) . . . . .	5-67
5-44	Assumed Shear Transfer Between Door and Fuselage for Model I . . . . .	5-67
5-45	Axial Load Distribution in Door and Fuselage Longeron . . . . .	5-67
5-46	Assumed Shear Transfer Between Door and Fuselage for Model II . . . . .	5-69
5-47	Equivalent Shear Panel to Represent Strain Energy in Straps and Longerons . . . . .	5-70
6-1	Stress Distribution Due to Uniform End Shortening . . . . .	6-4
6-2	Assumed Stress Distribution Due to Linear End Bending . . . . .	6-5
6-3	Fuselage Effective Skin Widths . . . . .	6-6
6-4	Method for Lumping Effective Panel Widths Into Equivalent Caps . . . . .	6-7
6-5	Effective Wing Skin Widths . . . . .	6-10
6-6	Local Springs to Account for Fin Connection Flexibility . . . . .	6-12
6-7	Local Fuselage Angular Distortion, $\theta_{FA}$ . . . . .	6-13
6-8	Payload Beam Static Load Case Showing Springs to be Added . . . . .	6-14
7-1	Static Test No. 3 - Stress and Deflection Correlation . . . . .	7-3

VOLUME II LIST OF ILLUSTRATIONS (Cont)

<u>Figure</u>		<u>Page</u>
7-2	Static Test No. 4 - Stress and Deflection Correlation . . . . .	7-4
7-3	Static Test No. 5 - Stress and Deflection Correlation . . . . .	7-5
7-4	Static Test No. 6 - Stress and Deflection Correlation . . . . .	7-6
7-5	Static Test No. 7 - Stress and Deflection Correlation . . . . .	7-7
7-6	Static Test No. 8 - Stress and Deflection Correlation . . . . .	7-8
7-7	Static Test No. 21 - Stress and Deflection Correlation . . . . .	7-9
7-8	Wing Bottom Cover Compressive Bending Stress (Model I) (Dead Load Included) . . . . .	7-10
7-9	Wing Static Deflection - (Run 13) Test and Analysis Comparison . .	7-11
7-10	Correlation of Payload Deflections - Static Test No. 26 . . . . .	7-12
7-11	Fuselage Section Property Curves . . . . .	7-13
7-12	Equivalent Trapezoidal Stress Blocks for an Assumed Nonlinear Stress Distribution . . . . .	7-14
7-13	Method Used to Obtain Experimental Influence Coefficients . . . . .	7-15
7-14	Normalized Mode Shape - First Symmetric Mode . . . . .	7-18
7-15	Normalized Mode Shape - Second Symmetric Mode . . . . .	7-19
7-16	Normalized Mode Shape - Third Symmetric Mode . . . . .	7-20
7-17	Normalized Mode Shape - Fourth Symmetric Mode . . . . .	7-21
7-18	Normalized Mode Shape - Fifth Symmetric Mode . . . . .	7-22

## VOLUME II LIST OF TABLES

<u>No.</u>		<u>Page</u>
2-1	Pertinent Scaling Relationships for the 1/8-Scale Model . . . . .	2-6
2-2	Summary of Load Factors Used in 1/8-Scale Model Design . . . . .	2-7
2-3	Design Weight Distribution for 1/2 of the 1/8-Scale Orbiter Model Structure . . . . .	2-8
3-1	Statistical Description of 1/8-Scale Orbiter - Model I . . . . .	3-9
3-2	NASTRAN Model Weights and Center-of-Gravity Locations . . . . .	3-20
3-3	Lowest Frequencies for Orbiter Substructures - Model I . . . . .	3-23
3-4	Frequencies for Symmetric and Antisymmetric Modes - Model I . . . . .	3-26
4-1	Summary of Measured Symmetric Free-Free Modes (Horizontal Inverted Orientation) . . . . .	4-8
4-2	Variation of Fundamental Frequency with Axial Preload . . . . .	4-8
4-3	Static Tests . . . . .	4-19
4-4	1/8-Scale Orbiter (Model I) Measured and Calculated Influence Coefficients . . . . .	4-20
5-1	Orbiter Substructure Contributions to First Symmetric Modal Mass and Stiffness (Model I) . . . . .	5-4
5-2	Results of Fuselage Beam Model Analyses. . . . .	5-17
5-3	Summary of Calculations for Simple Two-DOF Problem . . . . .	5-22
5-4	Convergence of Frequency Using Frequency-Dependent Reduction Transformation for Simple Two-DOF Problem . . . . .	5-24
5-5	Results of Error Bound Calculation for First Three Symmetric Fuselage Substructure Modes . . . . .	5-25
5-6	Summary of Forward Fuselage Analytical Investigations . . . . .	5-29
5-7	One-g Longerons Stresses, Orbiter Supported Inverted and Horizontally from Interstage Attachments . . . . .	5-34

VOLUME II LIST OF TABLES (Cont)

<u>No.</u>		<u>Page</u>
5-8	Selected Analysis and Test Results for First Free-Free Symmetric Mode . . . . .	5-35
5-9	Elastic Buckling Stresses for Simply Supported Side Wall and Bottom Deck Panels . . . . .	5-37
5-10	Elastic Buckling Loads . . . . .	5-37
5-11	Fuselage Moments of Inertia for Various Effectiveness Factors . . . . .	5-55
5-12	Estimates of Panel Imperfections . . . . .	5-56
5-13	Moment of Inertia Using Exact and Approximate Formulas for Sta 116.0 . . . . .	5-60
5-14	Parameters for Simple Torque Cell Calculations . . . . .	5-65
5-15	Torque Cell Effectiveness Factors and Rotations for a Unit Nose Torsion . . . . .	5-72
6-1	Typical Fuselage Section Properties at Sta 116.0 . . . . .	6-9
6-2	Local Spring Constants to Account for Fin Connection Flexibility . . . . .	6-12
6-3	Comparison of Analytical and Experimental Deflections . . . . .	6-15
6-4	Frequencies for Orbiter Substructures - Comparison of Models I and II. . . . .	6-15
6-5	Frequencies for Symmetric and Antisymmetric Modes for Models I and II. . . . .	6-16
7-1	Static Test Correlation . . . . .	7-2
7-2	Fuselage Influence Coefficient Correlation . . . . .	7-16
7-3	Comparison of Analytical and Experimental Frequencies for the Symmetric Free-Free Normal Modes . . . . .	7-17
7-4	Substructure Contributions to the Z Component of Momentum for the First Free-Free Mode for Model I and Model II . . . . .	7-23

VOLUME II LIST OF TABLES (Cont)

<u>No.</u>		<u>Page</u>
7-5	Estimated Stresses for Static and Dynamic Tests . . . . .	7-24
7-6	Selected Analysis and Test Results For First Free-Free Symmetric Mode . . . . .	7-25
8-1	Orbiter NASTRAN Analysis Computing Statistics . . . . .	8-4

VOLUME IIIA TABLE OF CONTENTS

<u>Appendix</u>		<u>Page</u>
A1	Design Drawings for 1/8-Scale Orbiter Model . . . . .	A1-1
A2	NASTRAN Model II Finite Element Idealization Showing Revisions to Model I . . . . .	A2-1
A3	Load-Deflection Curves from Static Tests . . . . .	A3-1
A4	NASTRAN Substructuring Analysis for Normal Modes - Revised ALTERED Rigid Format 3 for Phase 1 or 2 . . . . .	A4-1
A5	NASTRAN Executive Control Deck - Model II Analysis . . . . .	A5-1
A6	Input Bulk Data - Phase 1 Analysis: Model II Fuselage . . . . .	A6-1
A7	Plots of Member Data - Phase 1 Analysis: Model II Fuselage. . . . .	A7-1
A8	Plots of Symmetric Free-Free Modes - Phase 1 Analysis: Model II Fuselage. . . . .	A8-1
A9	Plots of Antisymmetric Free-Free Modes - Phase 1 Analysis: Model II Fuselage . . . . .	A9-1
A10	Sorted Bulk Data - Phase 1 Analysis: Model II Wing . . . . .	A10-1
A11	Plots of Member Data - Phase 1 Analysis: Model II Wing . . . . .	A11-1
A12	Plots of Symmetric and Antisymmetric Modes - Phase I Analysis: Model II Wing . . . . .	A12-1
A13	Sorted Bulk Data - Phase 1 Analysis: Model II Payload . . . . .	A13-1
A14	Plots of Symmetric and Antisymmetric Modes - Phase I Analysis: Model II Payload . . . . .	A14-1
A15	Sorted Bulk Data - Phase 1 Analysis: Model II Cargo Doors . . . . .	A15-1
A16	Plots of Member Data - Phase 1 Analysis: Model II Cargo Doors . . . . .	A16-1
A17	Plots of Symmetric and Antisymmetric Modes - Phase I Analysis: Model II Cargo Doors . . . . .	A17-1
A18	Sorted Bulk Data - Phase 1 Analysis: Model II Fin . . . . .	A18-1
A19	Plots of Member Data - Phase 1 Analysis: Model II Fin . . . . .	A19-1
A20	Plots of Symmetric and Antisymmetric Modes - Phase 1 Analysis: Model II Fin. . . . .	A20-1
A21	Input Bulk Data - Phase 2 Analysis: Model II Orbiter Including Copy Runs and Static Test Runs . . . . .	A21-1
A22	Plots of Symmetric Free-Free Modes - Phase 2 Analysis: Model II Orbiter . . . . .	A22-1
A23	Plots of Antisymmetric Free-Free Modes - Phase 2 Analysis: Model II Orbiter. . . . .	A23-1

## VOLUME IIIB TABLE OF CONTENTS

<u>Appendix</u>		<u>Page</u>
B1	NASTRAN Substructuring Analysis for Normal Modes - ALTERED Rigid Format 3 for Phase 1 or 2 . . . . .	B1-1
B2	NASTRAN Executive Control Deck - Model I Analysis. . . . .	B2-1
B3	Sorted Bulk Data - Symmetric and Antisymmetric Modes - Phase 1 Analysis: Model I Fuselage . . . . .	B3-1
B4	Plots of Member Data - Phase 1 Analysis: Model I Fuselage. . . . .	B4-1
B5	Plots of Symmetric Free-Free Modes - Phase 1 Analysis: Model I Fuselage . . . . .	B5-1
B6	Plots of Antisymmetric Free-Free Modes - Phase 1 Analysis: Model I Fuselage . . . . .	B6-1
B7	Sorted Bulk Data - Phase 1 Analysis: Model I Wing . . . . .	B7-1
B8	Plots of Member Data - Phase 1 Analysis: Model I Wing . . . . .	B8-1
B9	Plots of Symmetric and Antisymmetric Modes - Phase 1 Analysis: Model I Wing . . . . .	B9-1
B10	Sorted Bulk Data - Phase 1 Analysis: Model I Cargo Doors . . . . .	B10-1
B11	Plots of Member Data - Phase 1 Analysis: Model I Cargo Doors . . . . .	B11-1
B12	Plots of Symmetric and Antisymmetric Modes - Phase 1 Analysis: Model I Cargo Doors. . . . .	B12-1
B13	Sorted Bulk Data - Phase 1 Analysis: Model I Fin . . . . .	B13-1
B14	Plots of Member Data - Phase 1 Analysis: Model I Fin (Refer to Vol. IIIA, Appendix A19)	
B15	Plots of Symmetric and Antisymmetric Modes - Phase 1 Analysis: Model I Fin . . . . .	B15-1
B16	Sorted Bulk Data - Phase 1 Analysis: Model I Payload . . . . .	B16-1
B17	Plots of Symmetric and Antisymmetric Modes - Phase 1 Analysis: Payload (Refer to Vol. IIIA, Appendix A14)	
B18	Sorted Bulk Data - Phase 2 Analysis: Model I Orbiter . . . . .	B18-1
B19	Plots of Symmetric Free-Free Modes - Phase 2 Analysis: Model I Orbiter . . . . .	B19-1
B20	Plots of Antisymmetric Free-Free Modes - Phase 2 Analysis: Model I Orbiter . . . . .	B20-1

**ANALYTICAL AND EXPERIMENTAL  
INVESTIGATION OF A 1/8-SCALE DYNAMIC  
MODEL OF THE SHUTTLE ORBITER**

**Volume I - Summary Report**

**By P. W. Mason, H. G. Harris, J. Zalesak, and M. Bernstein  
GRUMMAN AEROSPACE CORPORATION  
Bethpage, New York 11714**

**INTRODUCTION**

The Space Shuttle configuration has more complex structural dynamic characteristics than previous launch vehicles, primarily because of the high modal density at low frequencies, and the high degree of directional coupling in the pitch plane. An accurate analytical representation of these characteristics is a primary means for treating structural dynamics problems during the design phase of the Shuttle program. The 1/8-scale model program was developed to explore the adequacy of available analytical modeling technology, and to provide the means for investigating problems which are more readily treated experimentally. The basic objectives of the 1/8-scale model program are to

- Provide early verification of analytical modeling procedures on a Shuttle-like structure
- Demonstrate important vehicle dynamic characteristics of a typical Shuttle design
- Disclose any previously unanticipated structural dynamic characteristics
- Provide for development and demonstration of cost-effective prototype testing procedures.

As originally proposed, the entire mated vehicle was to be analyzed using the NASA Structural Analysis System (NASTRAN). A separate mathematical model of each Shuttle model element was to be formulated and analytically mated with the other element mathematical models. However, difficulties arose during the investigation which have delayed completion of the mated-configuration analysis. These difficulties are related to the modeling procedures employed, deficiencies of the physical model, and present practical limitations of the NASTRAN program.



This four-volume report describes the analytical and experimental studies of the orbiter element of the 1/8-scale Shuttle model as listed in the FOREWORD. Studies pertaining to the External Tank and Solid Rocket Boosters are described in References 8-1 and 8-2, respectively.

## SYMBOLS AND ABBREVIATIONS

### Symbols

$\delta$	deflection, in.
$\delta_{ij}$	influence coefficient, i. e., deflection of point i due to unit load at point j., in./lb
$f_m$	frequency of model, Hz
$f_p$	frequency of prototype, Hz
$L_m$	length of model
$L_p$	length of prototype
t	skin thickness of model, in.

### Abbreviations

ALARM	}	computer programs to solve eigen-value problems of very large size
FEER		
ALTER		modification of NASTRAN rigid formats
CBAR	}	finite elements in the NASTRAN program used in analysis of Orbiter structure
CROD		
CSHEAR		
CTRMEM		
CQDMEM2		
CQUAD2		
DOF		degrees of freedom
ET		external Tank
GLOW		gross liftoff weight
LH <sub>2</sub>		liquid Hydrogen
LO <sub>2</sub>		liquid Oxygen
MPC		multiple point constraint - NASTRAN

<b>NASTRAN</b>	<b>NASA Structural Analysis System</b>
<b>SPC</b>	<b>single point constraint - NASTRAN</b>
<b>SRB</b>	<b>Solid Rocket Boosters</b>
<b>TPS</b>	<b>thermal protection system</b>

## DESCRIPTION OF PROTOTYPE SHUTTLE

The Grumman proposed Design 619 Space Shuttle, a 4.8-million-lb GLOW, 182-ft long, parallel-burn configuration, formed the prototype for the 1/8-scale model study. This particular Grumman design is shown schematically in the mated configuration, Fig. 1. The design includes an Orbiter, two Solid Rocket Boosters (SRB's) and an External Tank (ET). The ET consists of a monocoque  $\text{LO}_2$  tank, an intertank skirt with frames to accept SRB attachment members, and a  $\text{LH}_2$  tank with frames and skirts for SRB attachment.

The prototype SRB consists of a monocoque segmented steel cylinder providing the propellant carrying structure, a forward skirt with frames and longerons providing for interstage attachments, and an aft conical skirt with frames providing for interstage attachments and four longerons for the on-pad support structure.

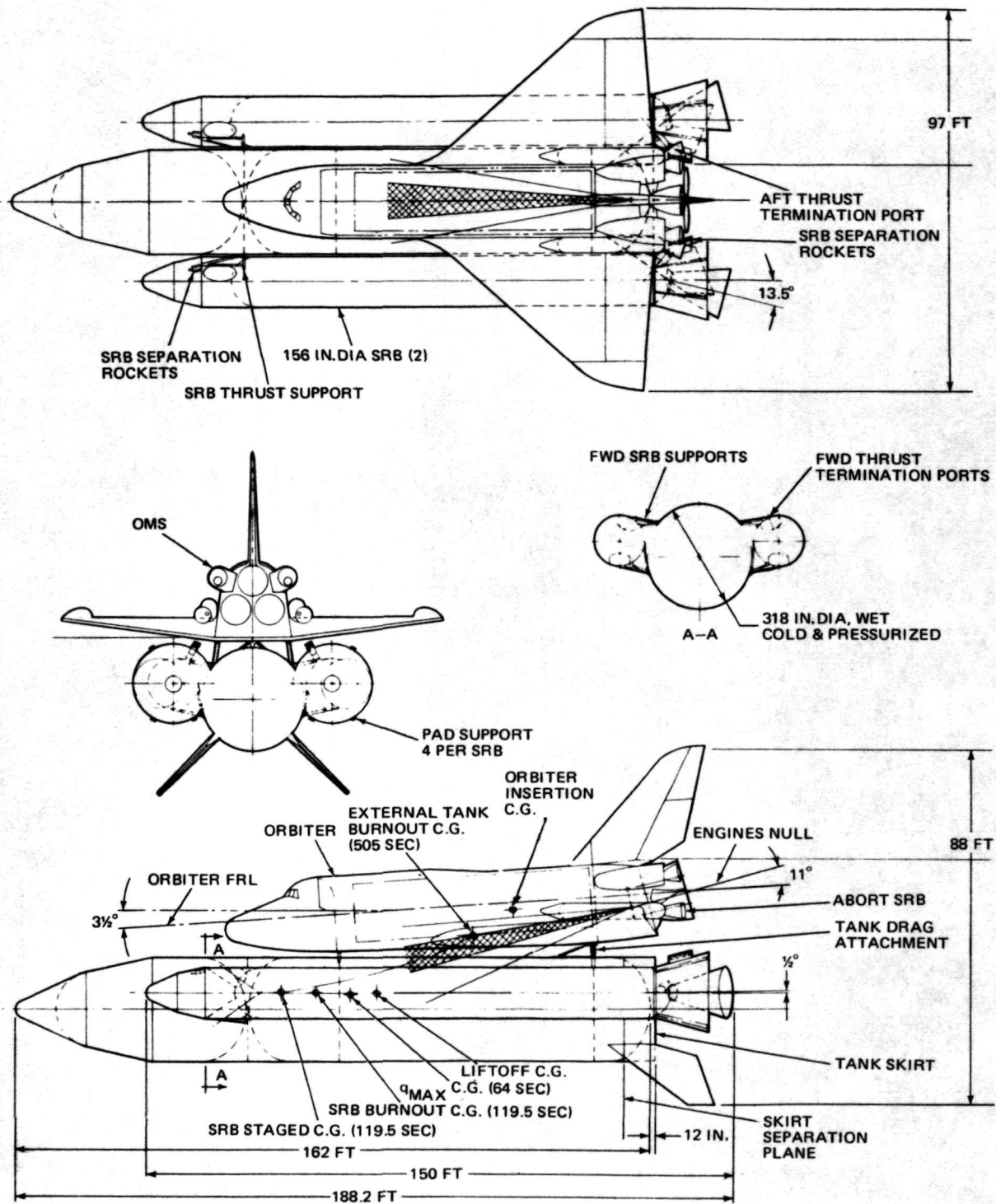
The prototype Orbiter consists of a forward fuselage module with the cabin life support system and controls, a U-shaped mid-fuselage with cargo bay doors, an aft-fuselage with engine thrust structure, delta wings with elevons, and a vertical fin. Figure 2 shows the structural arrangement of the prototype Orbiter.

After the 1/8-scale model design was completed, it was reviewed by Rockwell International, the prime contractor of the prototype Shuttle program. Under their sponsorship, an alternative configuration was designed for the portion of the model representing the forward attachment between the SRB and ET.

## DESCRIPTION OF 1/8-SCALE MODEL

The design philosophy for the present 1/8-scale orbiter dynamic model was to

- Derive from Grumman Design 619 an adequate model representing the significant low frequency characteristics for overall modes
- Maintain similarity of materials between the model and its prototype reference where feasible
- Meet an overall fabrication cost target.



S-1

Fig. 1 Grumman Parallel-Burn Space Shuttle Design 619 Used as Reference Prototype for 1/8-Scale Model Design

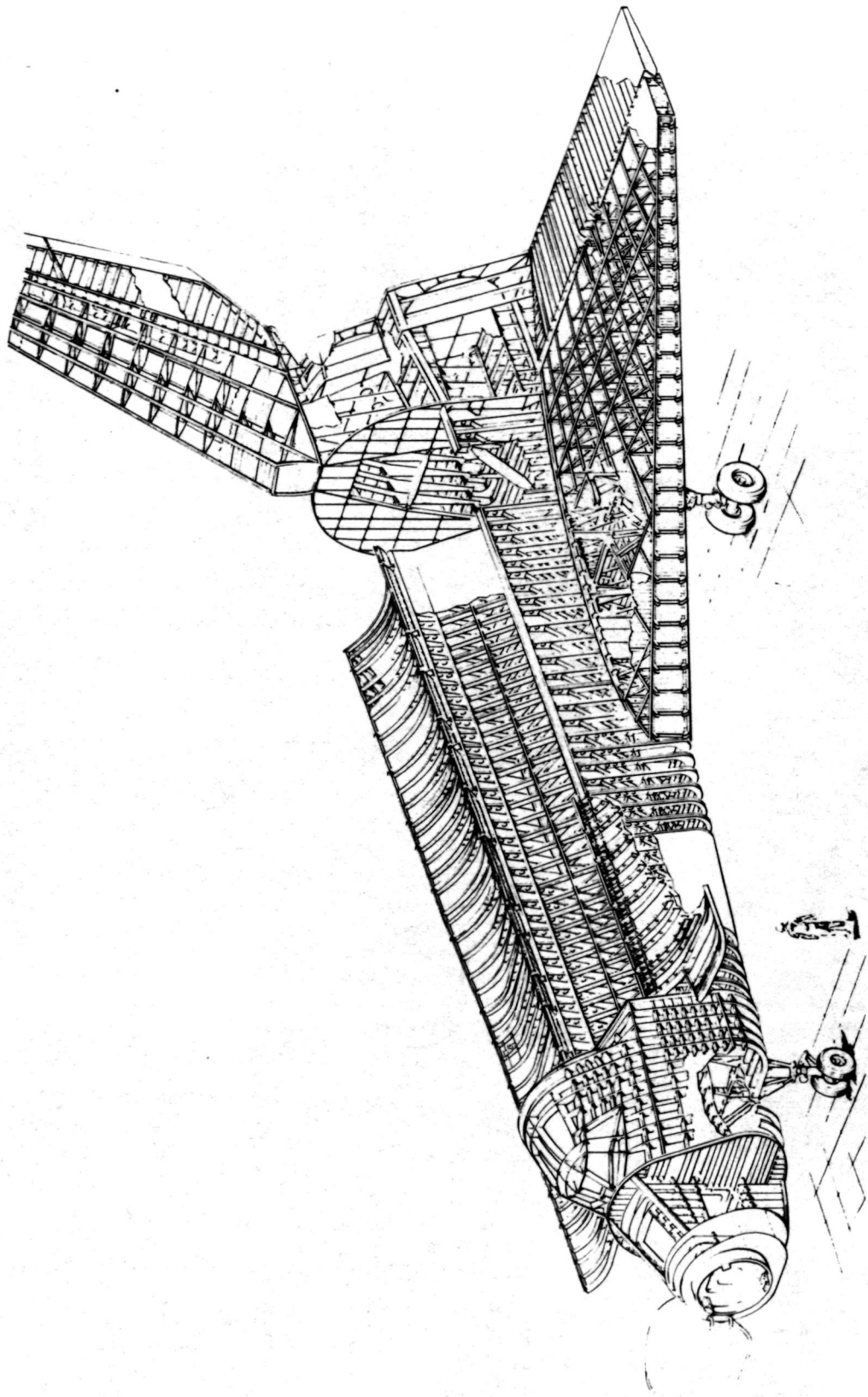


Fig. 2 Prototype Orbiter (Grumman Design 619) Structural Arrangement

Physical scale parameters of importance are listed in Table 1.

**Table 1. Summary of Significant Scale Factors**

Parameter	Expression	Scale Factor
Length	$L_m/L_p = 1/\lambda$	1/8
Weight	$W_m/W_p = 1/\lambda^3$	1/512
Material Density	$\rho_m/\rho_p = 1$	1
Frequency	$\omega_m/\omega_p = \lambda$	8
Material Modulus	$E_m/E_p = 1$	1
Poisson's Ratio	$\nu_m/\nu_p = 1$	1
Longitudinal Stiffness	$(EA)_m/(EA)_p = 1/\lambda^2$	1/64
Bending Stiffness	$(EI)_m/(EI)_p = 1/\lambda^4$	1/4096

ST-9

Simplifications, such as constant-thickness unstiffened skins in place of variable thickness skin-stringer-frame construction were used to reduce fabrication costs of the experimental model and to simplify mathematical modeling. Likewise, frames constructed of back-to-back channel elements and fittings constructed of bent sheet were used in place of more elaborate machined parts in the prototype. Figure 3 shows a mockup of the mated 1/8-scale Shuttle model suspended vertically. Figure 4 shows the structural configuration of the Orbiter model (without doors).

A detailed description of the orbiter model is given in Reference 8-3. A brief summary of the physical details is presented in the following paragraph.

The fuselage consists of a forward 20-in. long non-circular shell representing the cabin, a 102.5-in. long midsection containing the payload area and wing support structure, and a 20-in. long aft section providing a representative engine and fin support structure. Major bulkheads of stiffened sheet construction are located in the forward and aft sections. The midsection consists of a series of U-shaped frames spaced 10 in. apart in most instances. The Orbiter model sidewalls are constructed of 0.020-in. 2024-T3 aluminum sheet which is greater than the directly scaled thickness of 0.012 in. representing prototype sheet and smeared area of stiffeners. The use of a thicker gage model skin (to account for the larger local bending and extensional rigidity of the prototype stiffened construction) would have changed the mass-

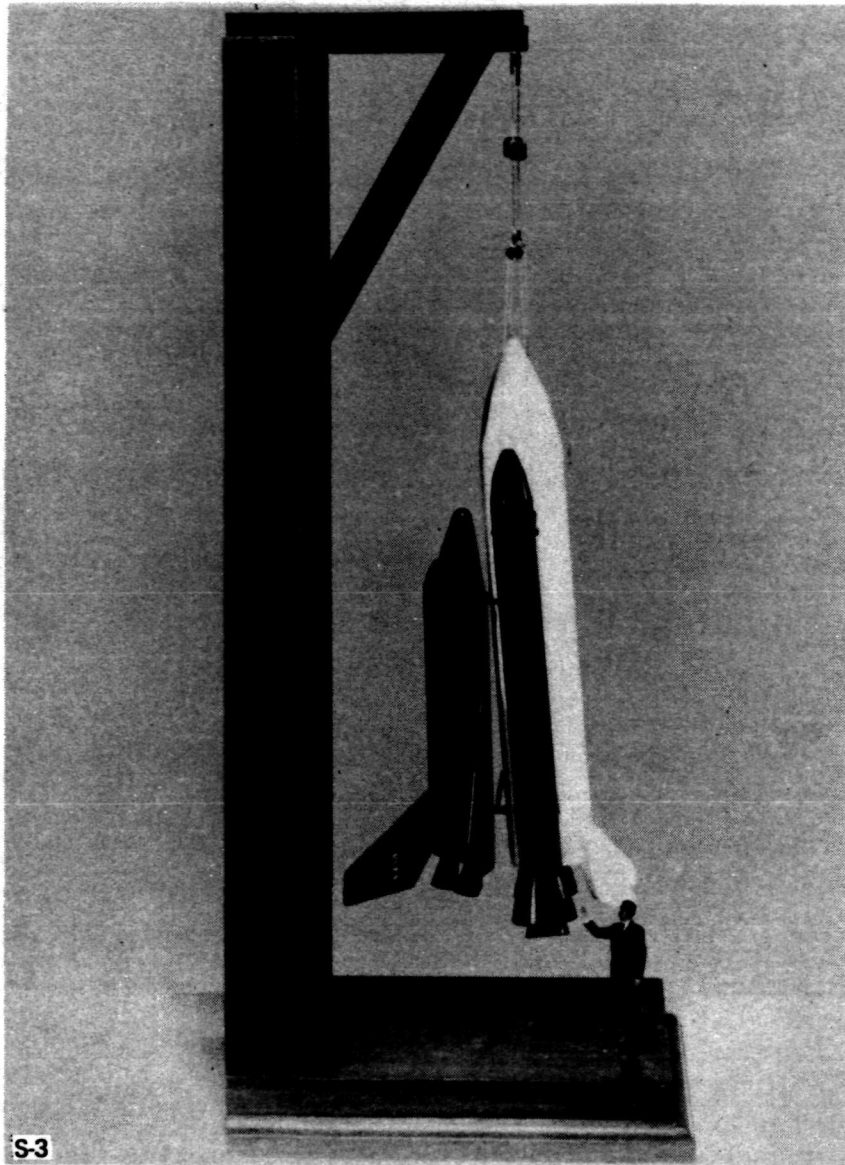
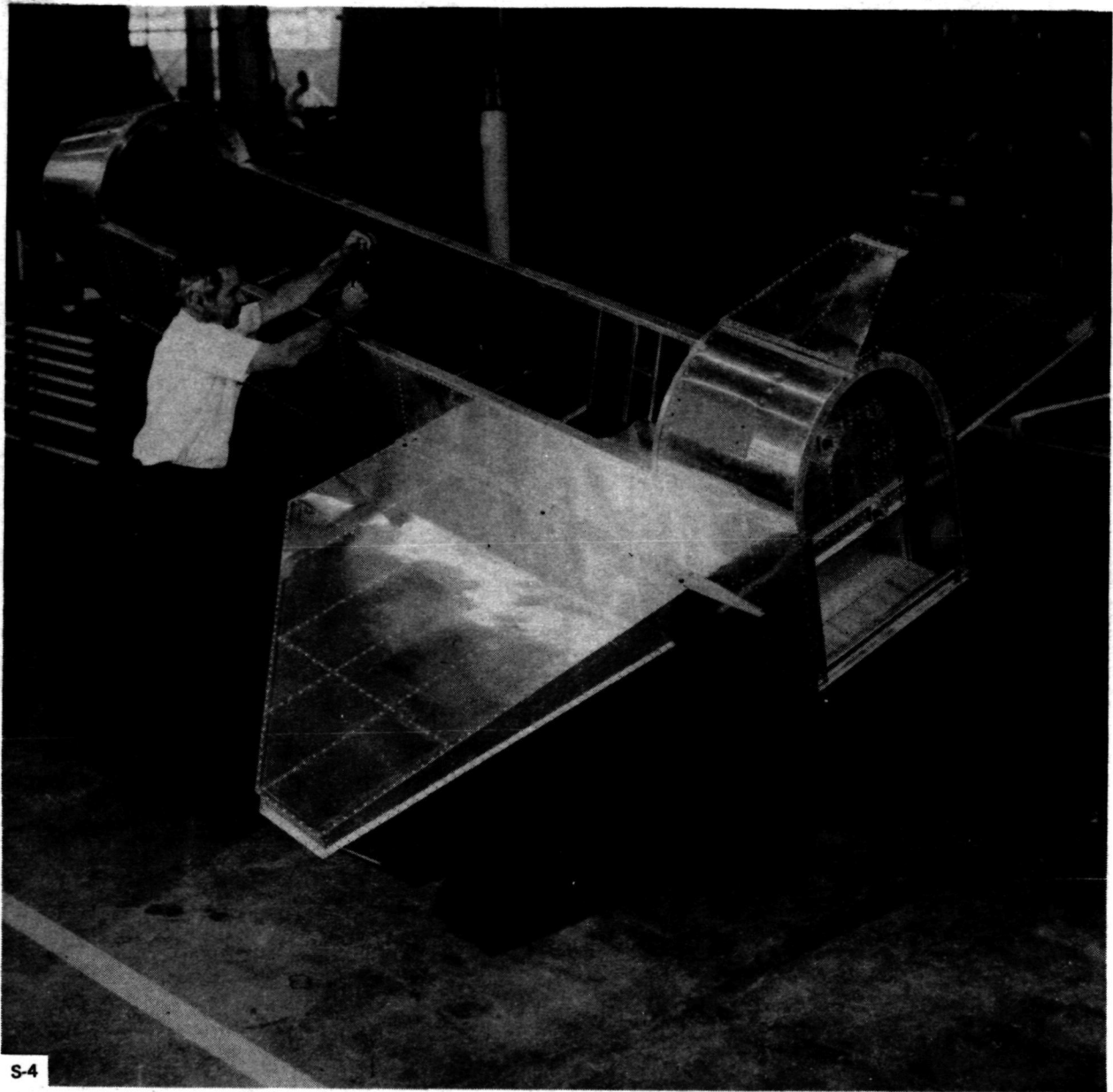


**Fig. 3 Mockup of 1/8-Scale Shuttle Model Basic Configuration**

stiffness ratios of model to prototype appreciably; the use of sandwich construction (although not considered seriously during design) would have increased the model cost substantially. The sidewall thickness of 0.020 in. (and bottom deck of 0.025 in.) would be sufficient to prevent elastic buckling, assuming an initially perfect flat plate. The wing skins are 0.020-in. thick sheet and the cargo door skins are constructed of 0.016-in. sheet.





S-4

Fig. 4 1/8-Scale Orbiter Model Structural Configuration

## NASTRAN FINITE ELEMENT MODELS

The mathematical modeling of the Orbiter began in January 1973. Consistent with the concepts of testing substructuring capability in NASTRAN level 15.5 (using ALTERS where needed), the structure was divided into five components: fuselage, fin, cargo doors, payload, and wing.

All skin material in the initial NASTRAN model (Model I) was considered to be nonbuckled, i. e., fully effective. This approach is consistent with the design of the full-scale Shuttle Orbiter where any wrinkling of the skins would loosen the bonded thermal protection system (TPS).

The total 1/2 Orbiter analytical model contained approximately 930 grid points and 2000 members. (Refer to Table 2.) Weight distributions for the 1/2 model are given in Table 3.

**Table 2. Statistical Description of 1/8-Scale Orbiter Model I**

Substructure	No. Grid Points	No. CBAR	No. CQDMEM2	No. CSHEAR	No. CROD	No. CTRMEM	No. CQUAD2	Total No. of Members	SYMM CASE		ANTISYMM CASE		
									DOF After SPC & MPC	DOF After GUYAN	DOF After SPC & MPC	DOF After GUYAN	
Payload	12	8	—	—	—	—	—	8	24	24	26	26	
Fin	59	—	24	22	65	—	—	111	101	25	99	24	
Wing	192	—	149	81	187	8	—	425	531	183	531	183	
Doors	134	9	20	64	178	—	16	287	396	26	384	26	
Fuselage	537	93	336	172	616	7	—	1224	1417	246	1368	222	
Total 1/2 Orbiter	934	110	529	339	1046	15	16	2055	2469	504	2408	481	
Orbiter Analysis ST-3	215	Contains 125 plotel elements								400	339	378	324

**Table 3. Design Weight Distribution for One-Half of the 1/8-Scale Model Structure**

Substructure	Weight, lb	Weight, %
Fuselage	100.91 <sup>(a)</sup>	48.34
Wing	32.86	15.74
Cargo doors	6.52	3.12
Fin	3.85	1.84
Payload	64.62	30.96
Total	208.76 <sup>(b)</sup>	100.00

<sup>a</sup>The fuselage weight of 100.91 lb contains the aft OMS ballast of 26.15 lb and the cabin ballast of 29.2 lb (per half structure)

TT-3 <sup>b</sup>The actual measured weight was 420 lb for the Orbiter Model

After the model had been fabricated and preliminary vibration tests started, disagreement between experimental and analytical data from Model I drew attention to bows in the fuselage sidewall and wing skins that were observed to be of the order of the sheet thickness. These initial imperfections are in line with simple calculated deadload deflections for a 9.5 x 16-in. sidewall panel, and a 9.5 x 12.5-in. bottom deck panel as shown in Table 4.

Subsequent experiments and analyses designed to resolve the disagreement verified that these initial imperfections increase the flexibility of the skins by as much as 50% (compared to perfectly flat sheet) in resisting in-plane axial and shear forces. Excessive flexibility was also observed to exist in the fin/fuselage connection. This resulted from a poor connection constructed of lower-cost sheet material, rather than a machined fitting. The cargo bay doors contain inherent built-in eccentricities in their connection to the fuselage. The original finite-element modeling did not adequately account for the behavior of these fittings and hence resulted in too stiff an analytical representation of the cargo door longeron. In addition, the forward/mid-fuselage splice contained more flexibility than the original finite element model. Likewise, the wing carry-through structure was built with a number of cutouts in the skins to facilitate fabrication, thus causing additional flexibility in the model in that region.

A number of experimental model design changes were proposed subsequent to fabrication and initial testing. The major fixes considered were stiffening the fuselage and wing skins with external hat stiffeners and changing the fin-fuselage attachment. These changes were not incorporated because:

- There was a lack of experimental data needed to positively ascertain the major problem areas and the extent of their contribution to the overall correlation
- The prime objective of the program was to analytically represent the existing physical model (shuttle-like) where feasible
- Suggested modifications of the experimental model would have caused drastic slippage in the program schedule with resulting delay in the exercise of NASTRAN capabilities.

**Table 4. Calculated Maximum Deflections for Typical Panel Under Own Weight with Various Boundary Conditions**

Calculation	Dead Load, $\delta/t$
● Sidewall Panel (t = 0.020")	
– Beam Strip	1.51
– Simply Supported Plate	0.93
– Clamped Plate	0.25
● Bottom Deck (t = 0.025")	
– Beam Strip	0.77
– Simply Supported Plate	0.344
– Clamped Plate	0.103
ST-1	

Instead, it was decided to modify the NASTRAN analytical model to account for the nonlinearities of the ineffective skin, and the additional flexibility of major Orbiter component connections.

After a subsequent series of static and dynamic tests, it was concluded that the NASTRAN model should be modified to account for initial imperfections and poor joint designs. These changes in the finite element model (NASTRAN Model II) accounted for additional flexibility in six major areas that are discussed in detail in Volume II. The changes include:

- Fin/fuselage supports
- Forward/mid-fuselage splice
- Cargo door attachments
- Wing carry-through structure
- Effective width of fuselage and wing skins
- Payload attachment.

The complete details of the original and modified math models are contained in Volumes II, IIIA, and IIIB. Complete listings of the NASTRAN bulk data containing the geometry, types of finite elements and gages are also given in Volumes IIIA and IIIB.

In Table 5 the frequencies for NASTRAN Models I and II are compared with test values. The effects of revising the model were substantial. The agreement between analysis and test is very good for the low frequencies, and as generally expected, discrepancies between theory and test become larger for the higher modes.

Table 6 gives a comparison of the analytical and measured antisymmetric free-free modes. (Only the first lateral bending mode had been measured at the time of writing of this report.)

To place the values of Table 5 into perspective, Table 7 and 8 compare the weight and frequencies of the 1/8-scale model with a Grumman analysis of the prototype Shuttle (current as of March 1973). Note that the prototype vehicle is generally heavier, and (in particular) the prototype fin is considerably heavier than the model fin. Therefore, the predicted prototype frequencies would be expected to be proportionately lower as they are generally shown to be in Table 8. However, the prototype payload and fin fore-aft modes occur at higher frequencies when compared to the models. This is probably due to excessive flexibilities in the model fin-fuselage and payload-fuselage connections. These model joints are not considered to be representative of the type found in prototype vehicle designs.

Table 5. Comparison of Analytical and Preliminary Experimental Results for the Symmetric Free-Free Normal Modes

Mode	Model I Freq, Hz	Model II Freq, Hz	Test Freq, Hz	Model II to Test % Error	Description
1	53.2	44.2	43.6	+ 1.4	Fuselage 1st bending
2	62.6	54.4	51.2 } 54.2 }	+3.2	Wing 1st bending (vs payload vertical)
3	75.2	63.0	58.2	+ 8.3	Wing 1st bending (vs aft fuselage vert)
4	108.5	80.2	80.1	+ 0.1	Fin fore-aft
5	-	103.5	104.1 <sup>(a)</sup> } 106.8 }	- 3.1	Payload - aft vertical
6	133.8	115.9	-	-	Payload fore-aft (vs fwd fuselage fore-aft)
7	162.3	121.5	-	-	Aft fuselage pitch
8	133.8	139.7	-	-	Wing 1st torsion (vs fwd fuselage fore-aft)
9	175.3	170.9	-	-	Fuselage 2nd bending & wing fore-aft
10	216.5	185.0	-	-	Wing fore-aft bending

<sup>a</sup>Questionable mode; very similar to 106.8 Hz mode, also not measured during the second survey on 1-3-74.

**Table 6. Comparison of Analytical and Experimental Results for the Antisymmetric Free-Free Modes**

Mode	Model I, Freq, Hz	Model II, Freq, Hz	Test	Model II Test, % Error	Description
1	52.9	42.2	43.5	-3.0	Fus 1st lateral bending
2	72.6	57.0	-	-	Wing 1st bending/thin lat bending
3	85.1	58.6	-	-	Fin lat bending
4	101.5	71.6	-	-	Forward fus torsion
5	92.0	78.9	-	-	Aft fus roll-yaw
6	135.3	103.5	-	-	Fus 2nd torsion/wing torsion

**Table 7. Weight Comparison of Grumman Design 619 Prototype and 1/8-Scale Model**

Substructure	512* x 1/8-Scale Model		Prototype*	
	lb	%	lb	%
Fuselage	54,940	51.46	73,600	59.4
Wing	16,800	15.74	15,131	12.2
Fin	1,970	1.84	2,884	2.3
Payload	33,100	30.96	32,500	26.1
<b>Total 1/2 Orbiter</b>	<b>106,810</b>	<b>100%</b>	<b>124,115</b>	<b>100%</b>

\*512 is the length scale ratio to the third power, i.e.,  $\left(\frac{L_p}{L_m}\right)^3 = \left(\frac{8}{1}\right)^3$

**Table 8. Comparison of Prototype and 1/8-Scale Model Dynamic Analyses with Test Results for Symmetric Free-Free Modes**

1/8 Scale* Model II	1/8 Scale* Test	Prototype**	Normal Mode Description
5.5	5.45	3.56	Fuselage 1st Bending
6.8	6.40	5.26	Wing 1st Bending
-	12.0	5.38	Payload Pitch
-	-	7.23	Payload 1st Bending
15.2	13.4	8.28	Fuselage 2nd Bending
7.9	7.26	11.97	Payload Fore-Aft
-	-	12.32	Aft Crew Comp. Trunion
14.5	13.0	12.59	Wing 1st Torsion
-	-	14.17	Fwd Crew Comp. Trunion
10.0	10.0	14.70	Fin Fore-Aft
-	-	15.40	Wing 2nd Bending
-	-	16.68	Fuselage 1st Longitudinal
-	-	18.00	Fuselage 3rd Bending
-	-	23.05	Fuselage 2nd longitudinal
-	-	24.62	Payload 2nd Longitudinal

\*Scale factor on frequencies for replica models if  $f_m/f_p = 8/1$   
 \*\* Results from Grumman analysis of prototype shuttle current in March 1973

## EXPERIMENTAL RESULTS

The first series of vibration tests were conducted with the model suspended on soft springs in an upside-down configuration (Fig. 5). The main objective of these preliminary tests was to determine the symmetric free-free modes of the Orbiter and compare them with the initial NASTRAN analytical results. Table 5 gives a summary of the first seven measured modes. These vibration results were verified by repeating the tests on the Orbiter when suspended in a nose-up position under 1-g and 2.5 g axial loading condition. The results of the nose-up vibration tests were practically identical to the upside-down tests.

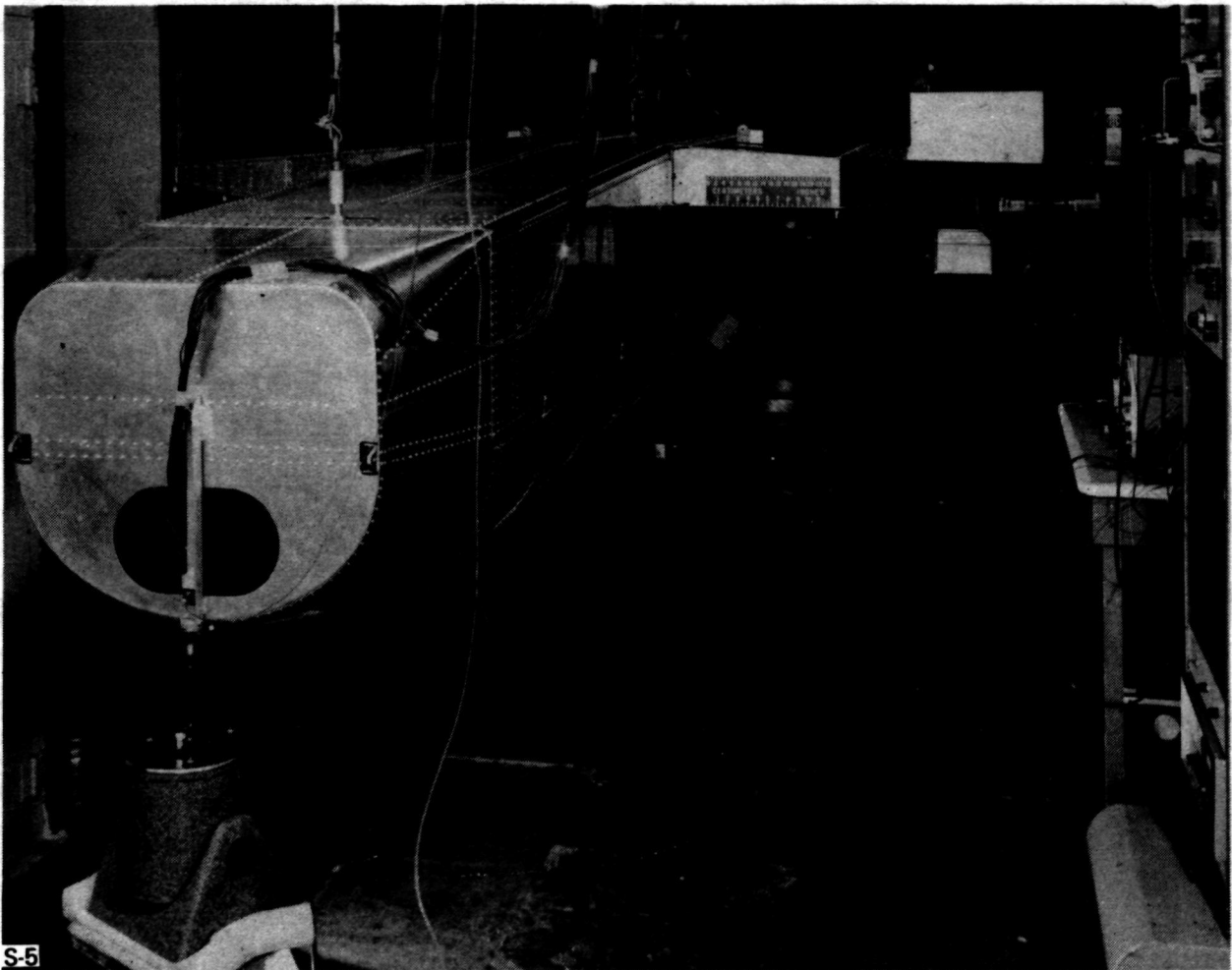
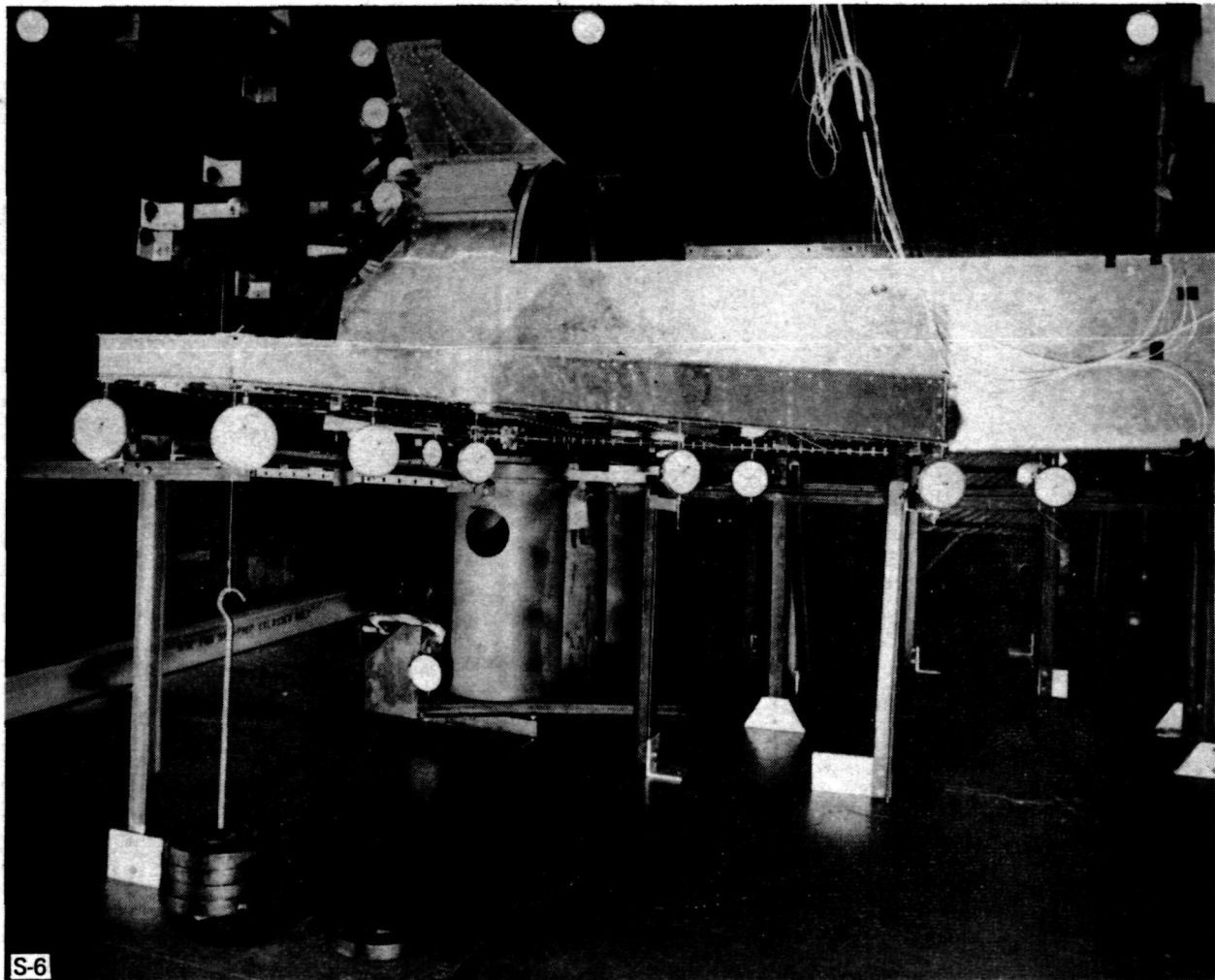


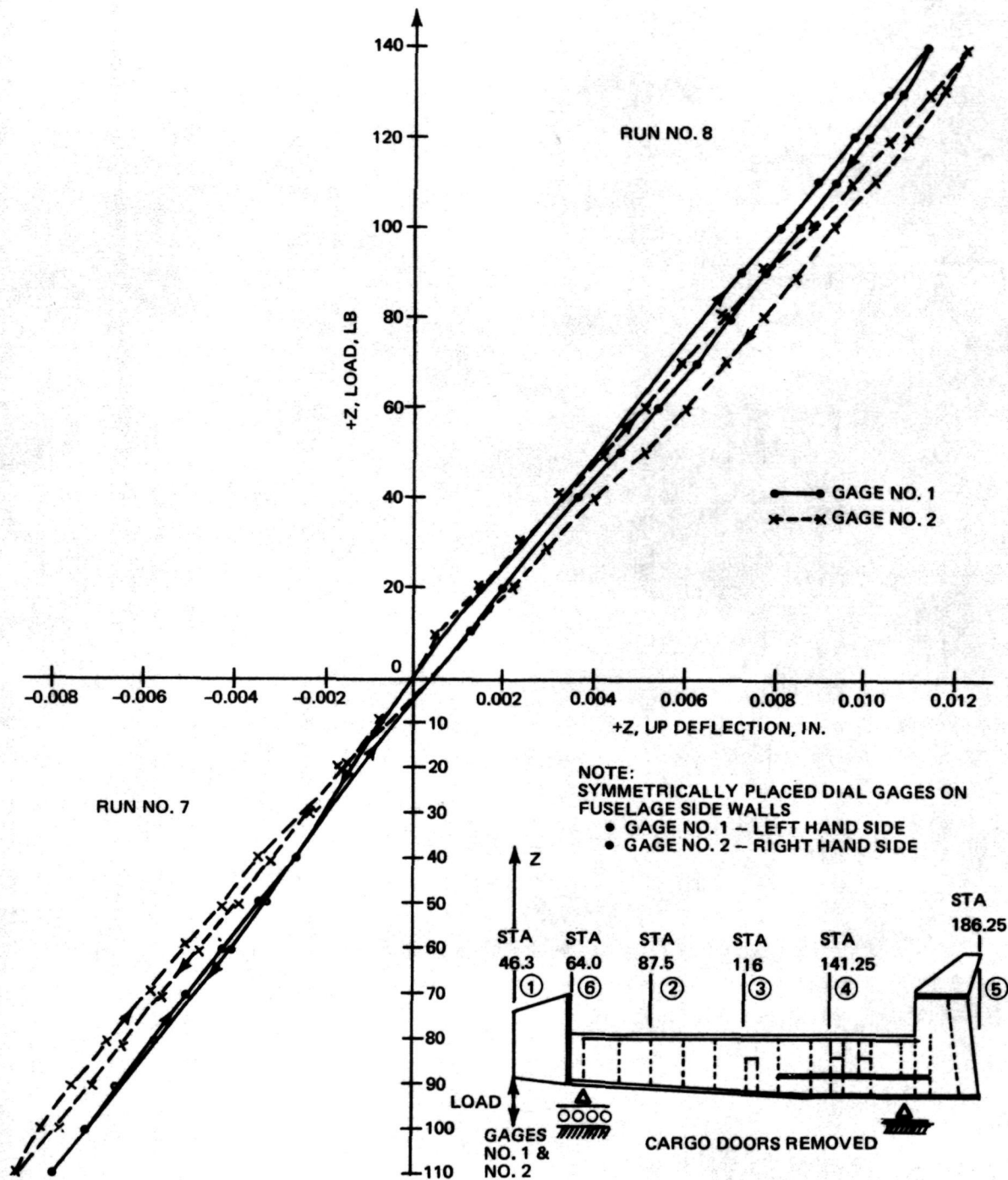
Fig. 5 Mode Survey of Model in Upside-Down Suspended Position

A series of static tests were conducted with the Orbiter model in a horizontal position, right side-up, supported at the interstage fittings, and loaded incrementally at a number of different locations (Fig. 6). Extensive deflection measurements were made over the whole surface of the model for each load case, during loading and unloading, to obtain influence coefficients for comparison with the analytical results. Figure 7 shows typical load-deflection curves for the transverse loading applied at the nose bulkhead. Table 9 summarizes the experimentally determined influence coefficients.



**Fig: 6 General View of Static Load Testing Arrangement of 1/8-Scale Orbiter Model**



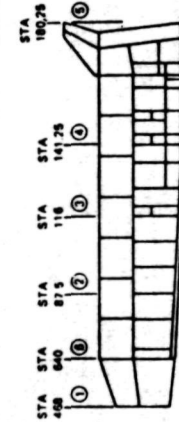


S-7

Fig. 7 Load Vs Deflection Curves for  $\pm Z$  Load on Nose Bulkhead

**Table 9 1/8 Scale Orbiter Model - Influence Coefficients**

Influence Coeff, In./lb	Mid-Fuselage Load, Cargo Doors On						Mid-Fuselage Load, Cargo Doors Off						Nose Load, Cargo Doors Off									
	Test Run 3, Down Load Sta 117.5		Test Run 4, Up Load Sta 116		Test Run 6, Down Load Sta 117.5		Test Run 5, Up Load Sta 116		Test Run 7, Down Load Sta 46.8		Test Run 8, Up Load Sta 46.8		NASTRAN Anal. Value Model		Test Run 7, Un-loaded		Test Run 8, Un-loaded					
	Model I	Model II	Avg	Un-loaded	Down	Up	Un-loaded	Avg	Un-loaded	Down	Up	Un-loaded	Avg	Model I	Model II	Un-loaded	Un-loaded	Avg				
1	2	3	4	5	6	7	8	9	10	11	12	13	14	15	16	17	18	19	20	21	22	23
δ13	-6.82	-14.19	-11.0	-8.9	-9.95	-7.4	-5.4	-6.4	-11.37	-10.1	-10.4	-10.25	-10.6	-14.0	-12.3							
δ23	18.14	25.76	24.7	23.8	24.25	21.3	20.8	21.05	22.03	26.2	27.9	27.05	24.6	27.0	25.8							
δ33	31.0	44.82	41.4	40.4	40.9	40.7	40.5	40.6	35.61	50.7	43.5	47.0	42.0	47.5	44.75							
δ43	17.94	25.32	26.3	26.0	26.15	27.0	23.8	25.4	21.99	28.0	24.0	26.0	26.5	28.8	27.65							
δ53	-11.28	-10.98	-11.28	-10.5	-10.95	-10.0	-8.5	-9.25	-15.04	-16.6	-13.0	-14.8	-10.4	-14.8	-12.6							
δ11																55.5	74.0	87.5	80.75	84.5	86.2	85.35
δ21																-5.0	-	-	-	-	-	-
δ31																-11.38	-8.5	-12.2	-10.35	-13.5	-10.8	-12.15
δ41																-7.6	-	-	-	-10.5	-7.8	-9.15
δ51																-4.78	-	-	-	-	-	-
δ61																19.16	-	-	-	31.5	34.5	33.0



Note: Values are based on slopes determined from preliminary data. Variations of approximately 10% are possible in interpreting the raw data and in repeating the tests.

TT-192A

## COMMENTS ON THE NASTRAN SYSTEM

The analysis of the 1/8-scale model was viewed as a pilot study of the use of NASTRAN on realistic aerospace projects. Therefore, some of the comments extend past specific application to the 1/8-scale model. Many areas must be considered in attempting to judge the NASTRAN system, some of which are not necessarily concerned with NASTRAN itself.

One of the prime reasons for Grumman's interest in NASTRAN is the work that NASA is doing in attempting to establish NASTRAN as the industry standard. For multi-corporation aerospace projects, standardization is a necessity. Standardization of computer programs, type of data, etc, is important from a contractual point of view, where subcontractors interface with prime contractors and the prime interfaces with the principal agency. However, with standardization there must be sufficient technical flexibility - in this regard NASTRAN has room for improvement.

### FLEXIBILITY OF THE NASTRAN SYSTEM

NASTRAN contains a number of rigid formats that allow for specific types of problems to be solved. Where these formats do not fit the specific application, the rigid format may be changed with ALTERS. In analyzing the 1/8-scale Orbiter model, numerous ALTERS to rigid format 3 were made. The system was modified to handle substructuring using level 15.5. It was found that, although the basic system can be modified, it requires an extensive learning period to become sufficiently proficient with the system to make use of ALTERS. After making a series of extensive ALTERS, the modified program must then be checked; if altered again, it must be rechecked. Because this procedure is cumbersome, it tends to produce a small group of NASTRAN experts. Our own in-house system (COMAP ASTRAL, Reference 8-4) contains no rigid formats; only one structural command generates all the required matrices (or those that are requested) to solve the problem. All matrix operations are coded in a simple, interpretive language that may be learned in a few hours. This system requires that the engineer understand the physics of the problem. Altering NASTRAN, on the other hand, requires a good understanding of the systems aspects of NASTRAN. Thus, there is diversion of engineering talent from engineering problem-solving to overcoming NASTRAN system complexities.

## CAPABILITY OF NASTRAN

The original analysis plan for the 1/8-scale model required that all components (Orbiter, ET and two SRB's) be coupled to determine mated vehicle modes. This combined hydro-visco-elastic analysis is theoretically possible within the present NASTRAN system, but from a practical standpoint it is not. Although we successfully calculated modes for the individual components, we were not able to couple these components and analyze the total vehicle due to extremely large computer time requirements. Note that the lack of correlation of the Orbiter analytical and test modes for Model I is not a fault of NASTRAN. This lack of agreement did, however, cause us to shift our emphasis from studying the coupling problem to examining the Orbiter modeling, design, and fabrication in more detail. Having cleared up the Orbiter correlation by the use of Model II, the coupling problem is still a major obstacle. Two approaches seem feasible:

- Modal coupling in lieu of static coupling to reduce the size of the final problem
- Incorporation into NASTRAN of approximate reduction schemes that employ the automatic tri-diagonal reduction algorithm. (For example, FEER, Ref. 8-3; or ALARM, being developed by Grumman under Master Agreement NASI-10635, Task 17. FEER and ALARM would have to be extended to handle complex modes.)

Master Agreement NASI-10635, Task 21 will pursue the modal coupling approach by making the appropriate ALTERS to the NASTRAN rigid formats.

Many complaints of NASTRAN are associated with the form of the stress output. Average stresses in elements are of little use to the engineer in the design mode. Traditional cap loads and shear flows are preferable. At this stage the designer is looking for the best load paths, and will rearrange the framing to the best of his ability to obtain it. The elements of a structure are proportioned to withstand the load imposed on them using allowable stresses, therefore the average stress in an element is not a convenient quantity. NASTRAN level 15.5 produces element corner forces which may be used as input to a post processor to produce equivalent cap loads and shear flows. The Grumman post processor produces listings of member loads not only by condition, but by critical condition ranking as well.

## CONCLUSIONS

Comments and recommendations concerning the analysis and correlation fall within four basic categories: the physical model, modeling procedures, correlation, and experiences with NASTRAN.

### PHYSICAL MODEL

One of the major constraints on the experimental model was the total cost of design and fabrication. It would have been better to place a cost on the total project: design, fabrication, analysis and testing. It is believed that through this study much has been learned about compromising fidelity in models to achieve simplicity. It is also apparent, in retrospect, that timely and careful attention during design to details and their associated effects on dynamic responses would have resulted in more desirable experimental model characteristics at justifiable costs. Thus, either a stiffened sheet or a sandwich construction could have minimized or eliminated the problems associated with the panel initial imperfections. Likewise, machined fittings would have eliminated the fin-fuselage connection problem.

### MODELING PROCEDURES

In NASTRAN Model I the CQDMEM2 element was used to model a fully effective structure. Lack of correlation should not be attributed to the behavior of this element or to NASTRAN. The major cause for lack of correlation was traced to the ineffectiveness of the skin panels due to the presence of initial bows. Model II used bars and shear panels to represent the behavior of the physical model. Here effective bar areas and an effective shear modulus were used. It is felt that this type of modeling is more descriptive of the actual characteristics of the structure. The effectiveness factors were obtained through the use of a computer program that solved the large deflection problem of in-plane loading of plates with initial imperfections. Little information exists in published form that contain the parameter range and type of loading of interest to the present study. Work was done by NASA some 20 years ago. It is recommended that this work be updated to cover a broad range of aspect ratios, initial imperfections and loadings. Publications of these data in chart form would be beneficial to modeling efforts on many structural projects.

Some remodeling of major joints could have been made in the analysis. However, for some joints such as the fin-fuselage connection, only static tests could give the exact behavior no matter how careful an analysis was made.

Consistent mass concepts tend to lose their significance for structures that do not behave in a linear fully effective fashion. In fact for structures of this type it becomes desirable to control the mass and stiffness properties independently.

#### CORRELATION

- The results of the vibration tests reported here are only preliminary, and have not been fully completed
- The static test data have a  $\pm 10\%$  error in reproducibility
- It is felt that the agreement of Model II results with test data is sufficiently close to pursue a coupling analysis.

#### EXPERIENCES WITH NASTRAN

Existing eigenvalue routines in NASTRAN are inadequate to handle the large size problems that are associated with the coupled structure. Routines such as FEER or ALARM should be added and extended to include complex eigenvalue problems.

The five Orbiter substructures were coupled using NASTRAN level 15.5. No great difficulties were encountered in using NASTRAN to do this. However, the column partitioning vectors required in the MERGE instruction are somewhat awkward. The equilibrium checks that were incorporated in the analysis proved helpful in finding errors and in giving a high level of confidence to the results. For the 1/8-Scale Model, five substructures were combined to give the total structure. Multilevel substructuring does not appear to present any technical difficulties.

The learning period required to become proficient with the NASTRAN system is excessive. But, regardless of many objections, a Government/industry standard like NASTRAN is a necessity.

## REFERENCES

- 8-1 Bernstein, M., Coppelino, R., Zalesak, J. and Mason, P.W., "Development of Technology for Fluid/Structure Interaction Modeling of a 1/8-Scale Dynamic Model of the Shuttle External Tank (ET)," NASA CR 132549, Grumman Aerospace Corporation, Bethpage, New York, June 1974.
- 8-2 Levy, A., Zalesak, J., Bernstein, M., and Mason, P. W., "Development of Technology for Modeling of a 1/8-Scale Dynamic Model of the Shuttle Solid Rocket Booster (SRB)," NASA CR 132492, Grumman Aerospace Corporation, Bethpage, New York, July 1974.
- 8-3 Anonymous, "Design of a Space Shuttle Structural Dynamics Model," NASA CR 112205 and CR 112205 Rev. A, Grumman Aerospace Corporation, Bethpage, New York.
- 8-4 Anonymous, "Grumman IDEAS Manual," Vol IIA, Grumman Aerospace Corporation, Bethpage, New York, April 1969.
- 8-5 Newman, M. and Pipano, A., "Fast Model Extraction Via the FEER Computer Program," Paper presented at the Third NASTRAN User's Colloquium, NASA/Langley Research Center, Hampton, Va., September 11-12, 1973, also NASA TMX 2893, September 1973, pp. 485-506.
- 8-6 Bernstein, M., Mason, P. W., Zalesak, J., Gregory, D.J., and Levy, A., "NASTRAN Analysis of the 1/8-Scale Space Shuttle Dynamic Model," Paper presented at the Third NASTRAN User's Colloquium, NASA/Langley Research Center, Hampton, Va., September 11-12, 1973, also NASA TMX-2893, September 1973, pp. 169-241.

**GRUMMAN AEROSPACE CORPORATION**  
BETHPAGE, NEW YORK 11714

1504-74